Core-level processes in the electron-stimulated desorption of CO from the W(110) surface

J. E. Houston* and Theodore E. Madey
Surface Science Division, National Bureau of Standards, Washington, D. C. 20234
(Received 14 December 1981)

Franchy and Menzel recently reported a significant increase in the electron-stimulated desorption (ESD) yield of O^+ ions from CO adsorbed on the (100) surface of W at 120 K when the incident-electron energy exceeded that necessary to excite the oxygen 1*s* core level. Disintegration of the adsorption complex which becomes multiply charged by Auger decay of the core hole was offered as an explanation. In the present work we have investigated this effect in detail for adsorption of CO at 80 K on the W(110) surface. In agreement with Franchy and Menzel, we observed an increased O^+ ESD yield for electron energies above the O 1*s* threshold for saturation coverages of CO adsorbed at 80 K. In addition, we find that the O^+ yield in this region is strongly dependent on coverage and post-adsorption thermal annealing. We present data which indicate that, in fact, the magnitude of the O^+ yield for electron energies much greater than the threshold appears to be rather insensitive to the CO binding site and follows closely the total CO coverage. In contrast, it is found that the O^+ yield from excitation processes which have their thresholds at low energies, i.e., less than 100 eV, is strongly dependent upon the chemical state of the adsorbed CO and is greatly suppressed for coverages above about 0.5 monolayer. The O^+-ion kinetic-energy distribution for excitation energies less than the O 1*s* threshold is found to peak at about 6 eV and cut off rapidly for energies less than approximately 3 eV, whereas for the high-energy desorption, i.e., for electron energies much greater than the O 1*s* threshold, the distribution extends to considerably lower ion kinetic energies. Coadsorption of $^{12}C^{16}O$ and $^{12}C^{18}O$ shows an isotope effect in ESD with yield ratio values of $^{16}O^+$ to $^{18}O^+$ equal to 1.6 ± 0.21 and $^{12}C^{16}O^+$ to $^{12}C^{18}O^+$ equal to 1.27 ± 0.027, which are found to be essentially independent of excitation energy (from 300—1000 eV). These results are discussed in the light of earlier work on this complex adsorption system.

I. INTRODUCTION

Electron-stimulated desorption (ESD), i.e., the removal of atomic and molecular species from surfaces by electron impact, has recently been the focus of increased attention, in part, due to the suggestion by Knotek and Feibelman[1] of the importance of core-level excitation as a means of supplying the local energy necessary for breaking surface bonds and to explain the degree of charge transfer that is often observed. This model specifically applies to desorption from maximal-valency oxide surfaces, i.e., oxides which leave the metal atom stripped of its valence electrons, and focuses on the interatomic Auger processes involving excited-metal core levels. Relaxation of the excited-metal core states proceeds through the removal of electrons from oxygen sites and O^+ (as well as other ionic species such as OH^+ and F^+) are desorbed due to the resulting reversal of the local Madelung potential. Although this model has called attention to the importance of core-level processes in ESD and has resulted in exciting new work using photon-stimulated desorption,[2,3] it has not provided a great deal of additional understanding of ESD from systems in which the bonding is substantially covalent.

ESD has been extensively studied over the last twenty years using, for the most part, electron energies of value less than about 150 eV.[4,5] The generally accepted desorption mechanism in this work involves the electron excitation of valence electrons into antibonding states followed by deexcitation (reneutralization in the ion-desorption case), resulting in the desorption of neutral and ionic species.[6] The magnitude of the cross sections for both neu-

tral and ionic desorption have been found to be sensitive to the chemical state (bonding configuration) of adsorbed molecules.[7] The role of core-level processes in the earlier work, however, was not made clear. The measurements of threshold energies that were done concentrated on the initial threshold in the region between 10—30 eV where valence processes and shallow core excitations are difficult to separate.[4,5]

In recent work, Franchy and Menzel[8] report studies on the desorption of O^+ and CO^+ from CO adsorbed on the (100) surface of W which show a significant increase in the ion yields for electron energies above that necessary to excite the deep C 1*s* and O 1*s* core states. These authors explain their results in terms of a process analogous to the "Coulomb explosion" observed in molecules[8] where Auger decay and Auger cascades, resulting from the primary core-hole state, lead to an accumulation of positive charge on the excited-atom site and a subsequent bond breaking due to Coulomb repulsion. This system is highly covalent, and certainly does not fit the Knotek-Feibelman condition, but emphasizes the importance in ESD of core-level processes. In the present paper we expand on the Franchy-Menzel work with studies of the beam-energy-dependent behavior of O^+ and CO^+ desorbed from CO on W(110) as a function of coverage and annealing temperature. In addition, measurements of ion kinetic energies and the effect of isotopic mass on desorption intensity have been made. These results are discussed in conjunction with the large body of information available from earlier studies of the CO-W system in an attempt to establish a coherent model for the ESD threshold enhancement for this particular system. We demonstrate that the ESD O^+ yield for incident electron energies less than the O 1*s* threshold is very sensitive to the CO coverage and binding state on W(110), whereas the O^+ yield for energies much greater than the O 1*s* threshold is less influenced by binding-state variations.

II. EXPERIMENTAL

The experimental apparatus used in the present studies has been described previously[5] and consists of an ion-pumped ultrahigh vacuum chamber containing facilities for the measurement of electron-stimulated desorption ion angular distributions (ESDIAD), low-energy electron diffraction (LEED), Auger electron spectroscopy (AES), and mass-resolved electron-stimulated desorption. In addition, the sample can be ion bombarded and its temperature varied from 80 K to greater than 2000 K by liquid-nitrogen cooling and resistive heating. The sample temperature can be continuously monitored by a W—3 wt. % Re vs W—25 wt. % Re thermocouple.

A focused electron beam (50—2500 eV) was generated in an electron gun, passed through a drift tube, and impinged on the sample surface with a beam diameter of $\lesssim 0.5$ mm and typical currents of $\sim 10^{-7}$ A. The sample could be rotated such that the desorbed ions resulting from electron bombardment could be viewed either by the ESDIAD apparatus or a quadrupole mass analyzer. In addition, the sample could be further rotated to face the coaxial gun of a cylindrical mirror analyzer for AES measurements and calibrated molecular-beam dosing arrangement for surface exposures to various gases.

The experiments were performed on a tungsten single crystal 7 mm in diameter which was cut in the form of a truncated pyramid such as to expose five separate facets.[9] The central facet was oriented to within 0.3° of the (110) plane and the four surrounding facets were stepped surfaces of varying step densities [6° and 10° off of the (110) plane]. The facets were cut such as to yield step orientations parallel to the [100] and [110] directions. This crystal was used in a previous study of oxygen adsorbed on W surfaces and has been described in detail in Ref. 10.

The sample was cleaned by flashing first to ~ 2000 K in a background of oxygen exposed directly to the sample surface as a molecular beam. This beam was formed by a microchannel plate array doser giving rise to a chamber background pressure of 4×10^{-8} T. The doser was operated in an uncalibrated mode but is estimated to have produced surface exposures equivalent to approximately 100 times that of the oxygen background pressure. The background oxygen was then removed from the chamber and the sample flashed to ~ 2300 K to remove the surface oxygen. This procedure was repeated monitoring the surface cleanliness by both AES and ESDIAD until negligible impurity indications using both methods were obtained. The ESDIAD, which utilizes a channel-plate electron multiplier array for observing the angular distribution of species desorbed from the surface under electron bombardment, was found to be extremely sensitive to certain species of surface

contamination not detected using AES, e.g., hydrogen and fluorine which were found to desorb as H^+ and F^+.

The measurements of ESD ion yield were made with the sample facing a quadrupole mass spectrometer. In measurements of the ion angular distributions it was found that for the CO-W(110) system both CO^+ and O^+ maximum yields occurred in directions parallel to the surface normal[11] and all measurements reported here were made with the axis of the mass analyzer parallel to this direction. In addition, the extent of the ion angle spread was compressed to a considerable degree by placing a + 50-V bias on the sample.[5] The electron gun filament voltage could be swept in a sawtooth form from 0—1500 V, which resulted in incident electron energies at the sample surface of from 50—1550 eV (uncorrected for filament work function). The sample current was recorded in order to normalize the resulting ESD intensity data with respect to electron flux.

The mass spectrometer was operated in a counting mode achieving count rates which varied from tens to thousands of counts per second. At these low ion current levels, the mass analyzer was set to read one particular mass component and the results were signal-averaged over several energy sweeps. In order to minimize electron-beam damage of the adsorbate layer, the electron-beam position was mechanically rastered, after a small number of voltage scans, in a rectangular array over the sample surface, i.e., the sample was translated under the stationary beam. This procedure was repeated until a sufficient signal-to-noise ratio was achieved. The resulting data was subsequently normalized with respect to both the number of scans and the beam-current value at each particular energy. A clean surface background was found resulting from electron-induced x-ray emission and this also was averaged and subtracted from the energy-dependent ion-yield data. Measurements of relative ion yield, e.g., O^+ relative to CO^+, as a function of beam energy, temperature, and exposure were obtained by signal-averaging multiple mass scans over the region of interest and subsequently integrating the resulting spectra.

Much of the present work was done on surfaces which had been exposed to the saturation CO coverage level and, as mentioned earlier, this was accomplished with a beam doser in order to minimize background chamber-pressure excursions. Relative coverages for the various exposure levels, which involved bleeding CO directly into the chamber to pressure levels monitored by a normal ion gauge, were determined by AES measurements of the carbon and oxygen signal intensities measured in the dN/dE mode. Because of the rapid electron damage resulting from exposure to the beam during Auger measurements, these data were again averaged over a small number of scans at each sample position while rastering the sample in a rectangular array under the electron beam.

The ion energy distributions were measured by placing a positive voltage on a planar grid located just before the ionizer section of the quadrupole mass spectrometer.[5] This retarding voltage was then swept with a sawtooth wave form and the quadrupole count rate for a particular ion mass was averaged over multiple scans. The distribution that resulted represented the integral of the ion energy distribution for that mass species (degraded, of course, by the instrument response function for the retarding arrangement). Measured ion energy distributions were obtained by transferring the data to a computer for smoothed differentiation.

The ion yields for two CO isotopes, i.e., $^{12}C^{16}O$ and $^{12}C^{18}O$ were accomplished by dosing a nearly equimolar mixture through a dual-manifold gas-handling system. After carefully baking these manifolds, approximately equal pressures (as measured by separate thermocouple gauges) of the two gases were admitted, one to each manifold. The manifolds were then opened to a central holding volume to obtain a nearly equal mixture of the two isotopes. Final evaluation of this mixture was obtained by bleeding it into the vacuum chamber and measuring the 28 to 30 mass ratio with the quadrupole analyzer. These measurements were again made in the signal-averaged and post-integrated mode described earlier. Only saturation dosages were used and this again was accomplished with the beam doser.

III. RESULTS

A. Dependence of ion yield on electron energy: saturation CO adsorbed at 80 K on W(110)

The results of measurements of O^+ and CO^+ ion yields from CO adsorbed to saturation coverages at 80 K on a W(110) surface as a function of electron energy are shown as the dotted curves in Fig. 1. These data have been corrected for beam-current variations and x-ray emission background and are compared directly with the results of Fran-

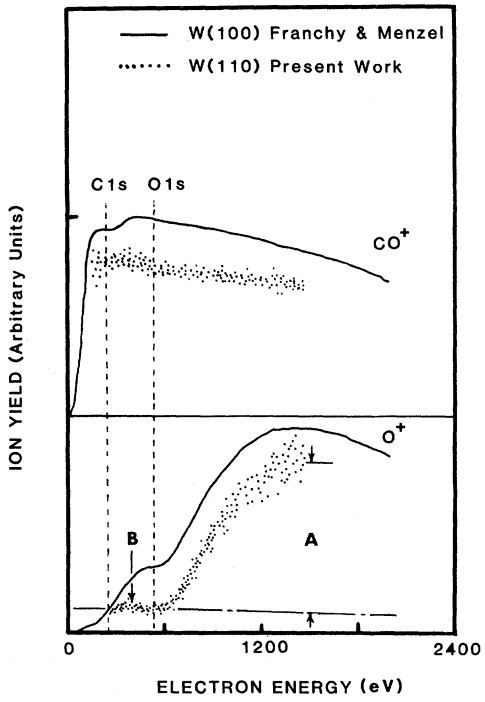

FIG. 1. Dotted curves represent data from the present work corresponding to O^+ and CO^+ relative ion yields for electron-stimulated desorption as a function of electron energy for CO adsorbed on the W(110) surface at 80 K. These data have been corrected for variations in incident-electron-beam current and for the background produced by x-rays. The solid curves are from earlier work by Franchy and Menzel (Ref. 8) and are for CO adsorbed on W(100) at 120 K.

chy and Menzel.[8] These latter data were taken at saturation CO coverages at 120 K on a W(100) surface and no mention is made concerning corrections for various experimental effects. The principal conclusion reached by Franchy and Menzel concerning the significant increase in the O^+ yield above the O 1*s* binding energy is certainly corroborated by our results. However, several differences in the data bear emphasis. First, in our corrected data, the degree to which the high-energy yield is increased over that found below the O 1*s* threshold is even more dramatic. Second, no clear increase in CO^+ yields above the C 1*s* is binding energy was detected reproducibly in our data. And finally, adequate low-energy data which was corrected for beam-current variations, could not be obtained in the present work because of the rapidly decreasing beam current below approximately 200 eV.

The significant increase in the O^+ yield above the O 1*s* threshold shown in Fig. 1 is rather unique to this particular adsorption state of the CO-W system as we will discuss later. A contrasting example of the behavior for another system is shown in Fig. 2 taken on a stepped W(110) surface exposed to saturation coverage of oxygen at ~ 1000 K. The solid line corresponds to uncorrected O^+-yield data and the dotted curve has been corrected for beam-current changes and the x-ray background. Here one notes a definite increase in O^+ yield above the O 1*s* threshold but to a degree which is considerably less (relative to the low-energy yields) than for the case of low-temperature CO adsorption. It is interesting to note also that these data could be obtained only from the stepped portions of the sample. The central (110) plane showed negligible O^+ emission following oxygen adsorption under these adsorption conditions, as reported earlier.[10]

A useful qualitative measure of the relative contribution to the ion yield resulting from electron energies above the O 1*s* threshold can be obtained by assuming that the ion-yield data consists of essentially only two distinct processes: (1) those having a low-energy threshold (below 100 eV) and (2) those having a threshold at or above the O 1*s*

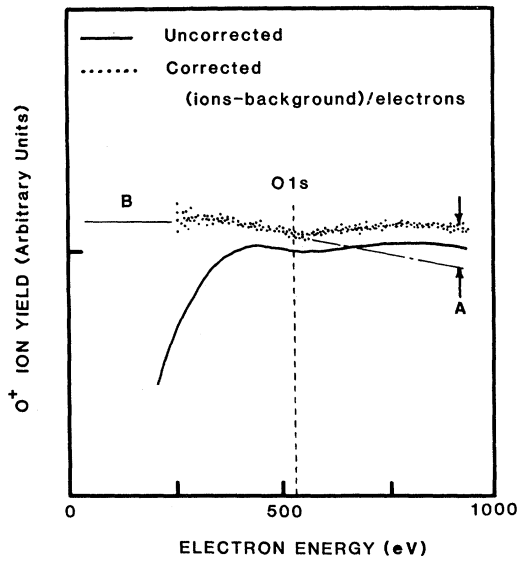

FIG. 2. Relative O^+ ion yields as a function of electron energy for an oxidized, stepped W(110) surface. The solid curve represents the raw data and the dotted curve has been corrected for electron-beam-current variations and the x-ray background.

binding energy. Above these threshold energies the yields are, then, assumed to follow a typical excitation cross-section behavior with respect to electron energy. The value of the yield at a given energy for the high-energy processes can then be calculated by extrapolating the energy behavior corresponding to the low-energy process to energies above the O 1*s* thresholds. An adequate approximation for this extrapolation can be obtained by using CO^+-yield data similar to that shown in Fig. 1. The result of this sort of analysis is that the CO^+ yield has a value of about 0.85 at $\sim$1500 eV relative to the value at $\sim$400 eV. Assuming that this figure is valid for the O^+ desorption the value of the O^+ yield resulting from the high-energy excitation can be calculated by subtracting from total O^+ yield at 1500 eV 85% of the total yield at 400 eV. This procedure results in the value indicated by the letter *A* in Fig. 1 whereas the value marked *B* is taken as indicative of the yield corresponding to the low-energy process. According to this procedure, the yield at 1500 eV is almost eight times that found for the low-energy process at 400 eV in the data of Fig. 1. In contrast, for the oxide data of Fig. 2 the yield at 950 eV is only about 15% larger than that found for the low-energy process at 400 eV.

B. Dependence of ion yield on CO coverage

Since it is known that the O^+ ion yield for CO adsorbed at low temperatures on other W surfaces varies rapidly with exposure,[12] it is of interest to determine if the O^+-yield ratio for the high- and low-energy excitation processes is itself related to exposure for CO on W(110). Our results for the variation of the O^+ yield with exposure for CO on W(110) at 80 K excited by 400-eV electrons are shown in Fig. 3 and these are in close agreement with those obtained by Yates and King for adsorption at 100 K on W(100).[12] As mentioned earlier, the relationship between exposure and coverage, relative to the saturation coverage value, can be determined by AES measurements, an example of which is given in Fig. 4 for CO exposures at 80 K. In Fig. 5, then, is shown the 400-eV O^+-yield data from Fig. 3 expressed as a function of relative coverage through the use of the results of Fig. 4. We include the O^+ yield versus exposure data of Fig. 3 because much of the data appearing in the literature is presented in this form and a direct comparison is thereby facilitated.

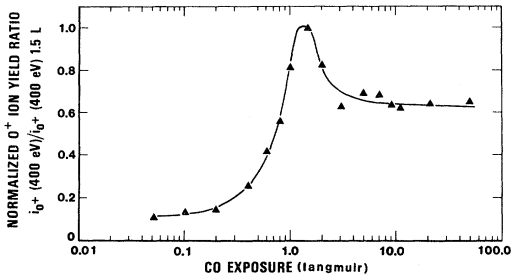

FIG. 3. O^+ ion yield plotted as a function of exposure, normalized to the yield value at a 1.5-L exposure, taken at 400-eV incident-electron energy for CO adsorbing on the W(110) surface at 80 K.

The behavior of the O^+ yield as a function of excitation energy plotted for several CO exposures at 80 K are shown in Fig. 6 corrected for incident electron current and x-ray background. Here one can see that the high-energy yield increases with exposure while that due to the low-energy process first increases and then decreases. This behavior can be followed in more detail by using the scheme for separating the low- and high-energy processes outlined earlier. Data of this kind are shown in Fig. 7 where the yield values have been calculated at 1500 and 400 eV and the data are plotted against relative coverage through the use of the calibration of Fig. 4. Also shown on Fig. 7 is the 100-eV CO^+-yield data obtained by Yates and King[12] placed on a relative coverage basis again through the use of our data of Fig. 4. The CO^+ yield has been scaled to agree with the CO^+:O^+ ratio found by Yates and King at an exposure of $\sim$1.2 L.

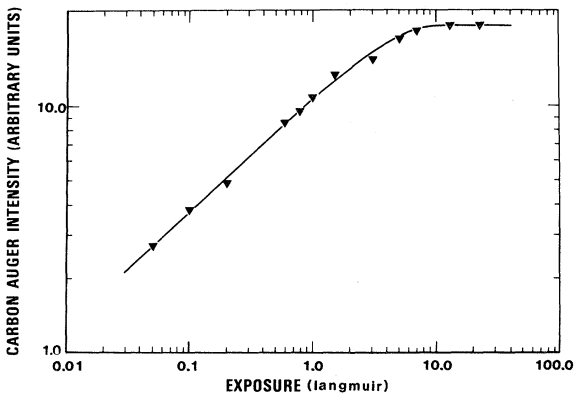

FIG. 4. Relative CO coverage plotted as a function of exposure for CO adsorbing on W(110) surface at 80 K. Relative coverages were measured as the peak-to-peak height for the carbon *KVV* Auger spectrum.

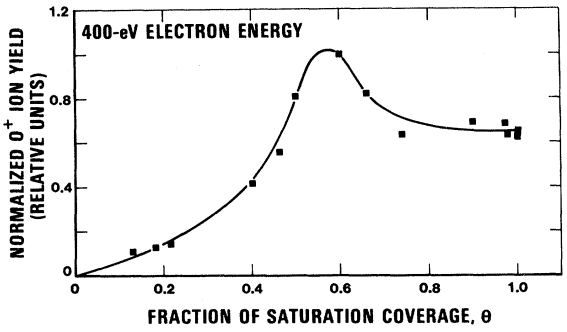

FIG. 5. O^+ ion yield of Fig. 3 plotted as a function of relative coverage through the use of the relative coverage vs exposure data on Fig. 4. The yield values have been normalized with respect to the value at a relative coverage corresponding to 1.5-L exposures.

C. Effect of temperature on ion yields

In addition to ion-yield variations with coverage, it is known that the ion yields are dramatically affected by temperature.[7] This behavior for both CO^+ and O^+ (with 400-eV excitation) for the thermal annealing of a saturation coverage of CO on W(110) at 80 K is shown in Fig. 8 and is in good agreement with earlier results[7,12] but differs from the recent work of Weng.[13] The behavior of the O^+ ion yield as a function of excitation energy for the post-adsorption annealing of a saturation coverage of CO on W(110) at 80 K is illustrated in Fig. 9, again separating the high- and low-energy processes by the scheme outlined earlier. Note that the dominance of the O^+ yield due to the high-

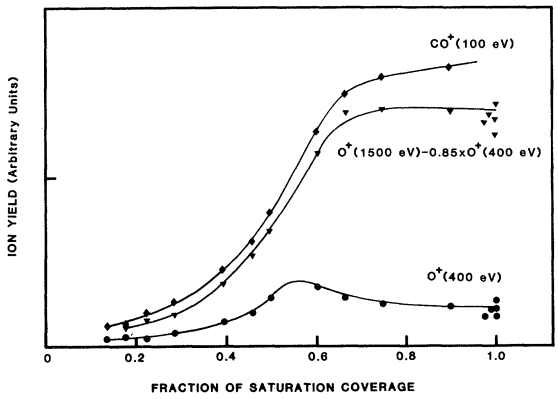

FIG. 7. Relative ion yields plotted as a function of relative coverage for CO adsorbing on W(110) at 80 K. The bottom curve represents the O^+ ion yield taken at an electron-beam energy of 400 eV. The middle curve represents the O^+ ion yield for the high-energy excitation processes calculated by subtracting 85% of the 400-eV yield from that measured at 1500-eV incident-beam energy. Top curve represents the CO^+ yield taken at 100-eV beam energy for CO adsorption on W(100) at 100 K from the work of Yates and King (Ref. 12). This latter data has been scaled to agree with our O^+ yield value at a coverage corresponding to 1.2-L exposure.

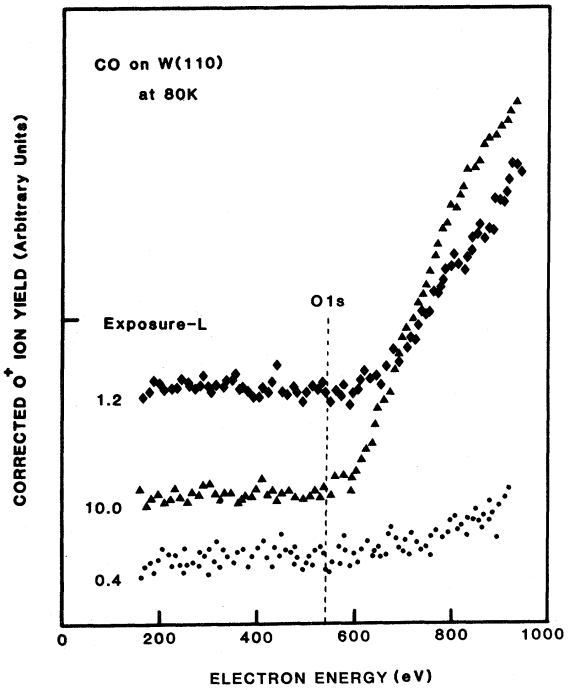

FIG. 6. Relative O^+ ion yields, corrected for incident-electron-beam-current variations and the x-ray background, as a function of electron-beam energy for three exposures, i.e., 0.4, 1.2, and 10.0 L of CO on the W(110) surface at 80 K.

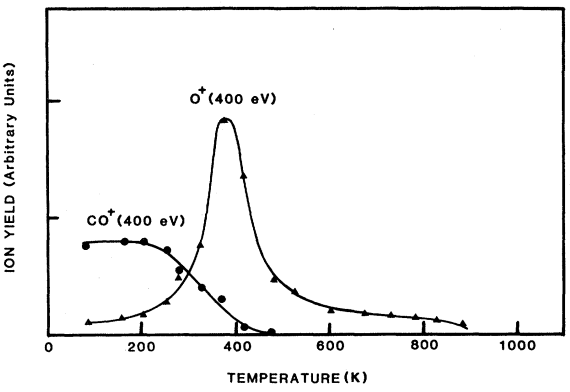

FIG. 8. CO^+ relative ion yields as a function of post-saturation-coverage annealing for CO on the W(110) surface. The initial exposure was done at 80 K and the data were taken at an incident-electron-beam energy of 400 eV.

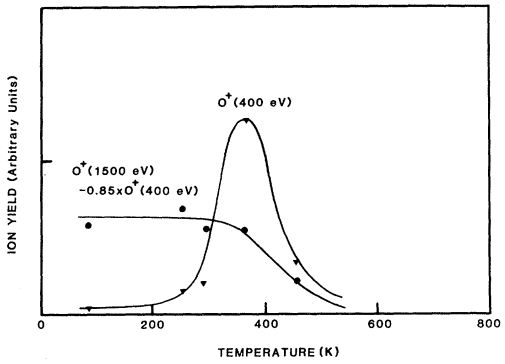

FIG. 9. Comparison of the O^+ ion yields as a function of post-saturation-coverage annealing for CO on the W(110) surface (initial exposure at 80 K) for the low-energy (400-eV) and high-energy excitation. The high-energy yield values are calculated as the yield at 1500-eV incident-beam energy minus 85% of that measured at 400 eV.

energy excitation is maintained to temperatures above 200 K. Thus, the data of Franchy and Menzel,[8] which were taken at 120 K, are seen to fall well within this region.

D. Ion energy distributions

In most models of the electron-induced desorption of ionic species,[1,6,8] reneutralization after excitation is visualized as playing a major role in determining ion yields. Thus, the time that an ion spends in the vicinity of a solid becomes a very important parameter. This time is, of course, related to the ion's velocity and, thus, to the strength of the interaction with the solid and to the ion mass. In the former case, the kinetic energy of the desorbed ion can yield valuable information concerning the details of the desorption mechanism.

In Fig. 10(a) is shown the ion kinetic-energy distributions of O^+ desorbed from the virgin CO layer (adsorbed to saturation at 80 K) compared directly for 400- to 1300-eV electron excitation. It is seen that the peak in the distribution for 400-eV excitation occurs at about 6 eV (uncorrected for the work-function difference between sample and retarding analyzer) and cuts off rapidly below this value. On the other hand, the 1300-eV excitation distribution (corresponding to large yield ratio between high- and low-energy excitations) peaks only weakly around 5 eV and has considerable intensity below 3 eV. The contrast between the saturated virgin CO case and desorption from the oxidized W(110) stepped surface is shown in Fig. 10(b).

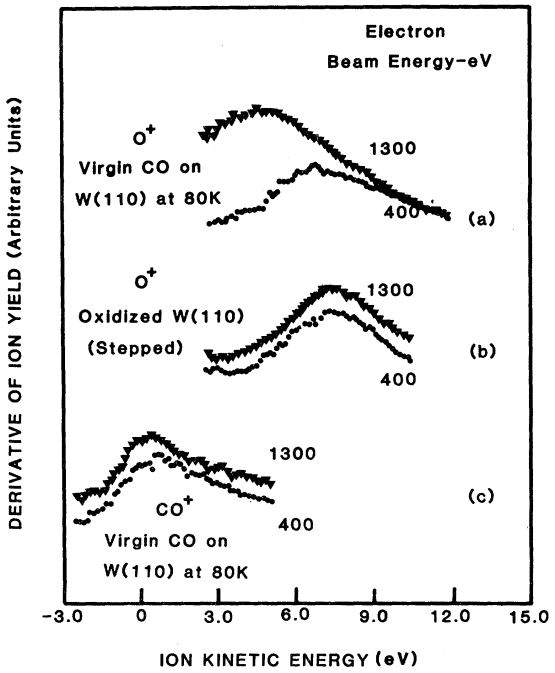

FIG. 10. Ion energy distributions comparing desorption with 400-eV electrons to that obtained with 1300-eV incident electrons. (a) corresponds to the desorption of O^+ from a saturation coverage of CO on the W(110) surface at 80 K, (b) shows similar data for O^+ emission from an oxidized, stepped W(110) surface, and (c) shows the CO^+ distributions for a saturation layer of CO on the W(110) surface at 80 K.

Here the distribution is somewhat similar to the virgin CO 400-eV curve, although it peaks at a slightly higher kinetic-energy value. The normalized distributions, however, do not show significant difference with the energy of excitation as is seen for the virgin case, which is in agreement with the results indicated in Fig. 2.

In contrast to the O^+ results, Fig. 10(c) illustrates the kinetic-energy distributions for the desorption of CO^+. For this case, the maximum desorption intensity appears to be near zero kinetic energy with the distribution extending to just above 3 eV. In addition, no significant differences with excitation energy can be detected, in agreement with our CO^+ results of Fig. 1. It shoud be noted in Fig. 10(c) that the energy distribution has nonzero values for negative kinetic energies. This behavior reflects the instrument response of the retarding analyzer. In fact, the distribution in this region can be viewed as approximately the integral of the instrument response function, which would

indicate an effective window width of just over 1 eV full width at half maximum (FWHM).

E. Isotope effect in the ESD of CO

Since under a given surface-adsorbate interaction the velocity of a desorbing species (and hence, the reneutralization time) depends upon its mass, the ion yield has been found to exhibit an isotope effect,[14,15] the study of which can add additional insight into the details of the desorption mechanism. For the virgin CO-W(110) system studied here, isotope data corresponding to $I_{^{16}O^+}/I_{^{18}O^+}$ and $I_{^{12}C^{16}O^+}/I_{^{12}C^{18}O^+}$ desorption as a function of incident-electron-beam energy are shown in Fig. 11 corrected for x-ray background. These curves represent the ratio of the corrected yields for isotopic ions plotted as a function of the energy of the incident electrons. The time required to accumulate this signal-averaged data (~1 h for each isotope ratio scanning point-by-point over the surface to minimize damage) is approximately the same for both the $I_{^{16}O^+}/I_{^{18}O^+}$ and $I_{^{12}C^{16}O^+}/I_{^{12}C^{18}O^+}$ results and, since the O^+ intensities are considerably less than those for CO^+, the signal-to-noise ratio is much less for the former relative to the latter. Two features of these data should be noted; first, the O^+ isotopic ratio is about 30% greater than that for CO^+ and, as expected, in both cases the light ion is favored. The second feature to be noted is the fact that within the confines of the noise no change in isotopic ratio could be detected with respect to excitation energy. The O^+ ratio values remain constant to within about 15% in spite of the fact that the O^+ yields themselves show a variation by approximately a factor of 6 over this same energy range.

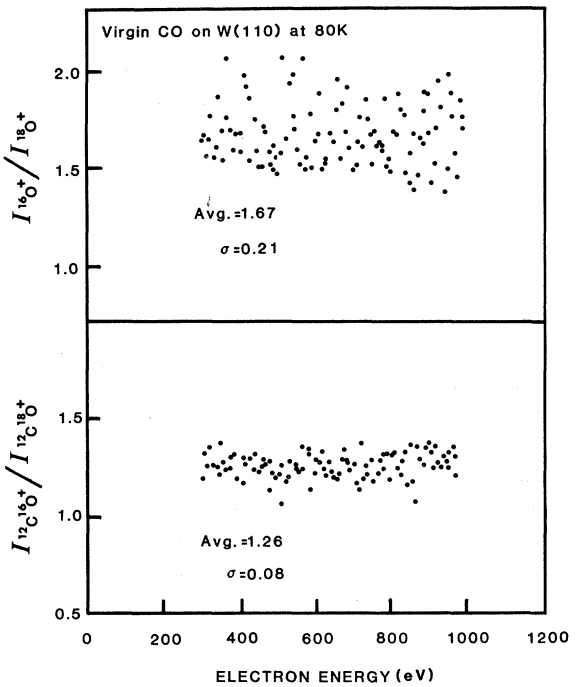

FIG. 11. Ion-yield ratios (corrected for x-ray background variations) for the saturation CO adsorption of $^{12}C^{16}O$ and $^{12}C^{18}O$ on the W(110) surface at 80 K as a function of incident-beam energy. The top panel shows the data for $I_{^{16}O^+}/I_{^{18}O^+}$ and the bottom panel corresponds to $I_{^{12}C^{16}O^+}/I_{^{12}C^{18}O^+}$. Values of the average yield ratio and its standard deviation are shown on each panel.

To better assess the variation of the isotopic yield ratios with excitation energy, we have calculated the average yield ratio values up to 500 eV and compared them with values calculated for energies above 500 eV. The calculations yield the following results:

$$I_{^{16}O^+}/I_{^{18}O^+}(<500\text{ eV})=1.68\pm0.22\ ,$$

$$I_{^{16}O^+}/I_{^{18}O^+}(>500\text{ eV})=1.67\pm0.21\ ,$$

$$I_{^{12}C^{16}O^+}/I_{^{12}C^{18}O^+}(<500\text{ eV})=1.25\pm0.065\ ,$$

$$I_{^{12}C^{16}O^+}/I_{^{12}C^{18}O^+}(>500\text{ eV})=1.27\pm0.075\ ,$$

from which we conclude that the isotopic yield ratios show negligible change above and below the O 1*s* threshold energy.

Previously Leung *et al.*[15,16] measured an ESD isotope effect at low electron energies for CO^+ desorption from virgin CO on W(110) and found that $I_{^{12}C^{16}O^+}/I_{^{12}C^{18}O^+}=1.6$. Their observation that the lighter isotope has the higher probability for desorption is in agreement with our results. The quantitative difference in values for the CO isotopic ratio may be due, in part, to ion optical effects in the two mass spectrometer detectors. Leung *et al.* did not report values for the $I_{^{16}O^+}/I_{^{18}O^+}$ presumably due to the low O^+ signal levels involved.

IV. DISCUSSION

A. Summary of the surface chemistry of the CO-W system

The adsorption of CO on tungsten has been one of the most intensely studied systems in surface

science and there are several excellent reviews covering work that spans more than 20 years.[7,17] One of the principal reasons for this continuing interest is the very complexity and variety of behavior that is exhibited in the results of a wide range of experimental techniques. Although a detailed review of the wealth of information available on the CO-W system is beyond the scope of the present paper, it is necessary to highlight this work in order to be able to place our results in proper perspective.

At temperatures below approximately 150 K, CO adsorbs on the W(110) surface in what Swanson and Gomer termed the virgin state.[18] Saturation coverage in this state is found to be approximately 0.8 of a monolayer and involves principally molecular CO standing upright with the carbon atom nearest the surface. The work function for this configuration is 0.6—1.0 eV higher than for the clean surface and the ESD ion yield at excitaton energies of 100—200 eV consists of largely CO^+ with a small amount of O^+. LEED studies of the W(110) surface indicate that a compression layer exists for coverage greater than 0.5 monolayer and a $p(5\times1)$ LEED pattern at saturation indicates that the CO structure is only slightly incommensurate with the W lattice in a nearly hexagonal close-packed structure with a coverage of 0.8 monolayer.[19]

Upon heating this saturated virgin layer several interesting effects occur and these are briefly summarized in Figs. 8 and 12. The ESD ion yields for low-energy excitation have already been presented in Fig. 8. The large initial CO^+ yield falls rapidly for temperatures above about 300 K with a commensurate rise in the O^+ yield. The O^+ then peaks near 400 K, subsequently reaching a plateau region above 600 K and finally disappears altogether near 900 K. The work-function behavior shown in Fig. 12(a) is seen to decrease rapidly in the same temperature region as the CO^+ yield, reaching a region of constant value above about 400 K and changing sign in the 900-K region.[7,16] Clean-surface work-function values are not achieved until about 1200 K. In thermal desorption [Fig. 12(b)] about 50% of the saturated coverage of CO is found to desorb in the temperature range from 200--400 K and the work-function fall corresponds closely with this desorption.[7,16,19] No further desorption occurs until above about 800 K and by 1200 K all adsorbed species are desorbed.

The state of the adsorbed species at temperatures in excess of 400 K is considered to be dissociative on the basis of experimental work involving isotopic mixing, LEED, UPS, and XPS (Refs. 7, 16, 17, and 20). The states which give rise to desorption for temperature above 800 K are usually referred to as the β states. The virgin state is generally considered to be entirely molecular in nature. Heating this layer to 300 K gives rise to some CO desorption and a partial conversion of the remaining CO to the β state. Further heating to 600 K, ensuring full β-state conversion, followed by readsorption at low temperatures produces what is referred to as the α state which is apparently a mixture of molecular and dissociated species.[7] Readsorption under this condition involves amounts approximately equal to the coverage of the β state remaining after the initial anneal. If, on the other hand, adsorption is carried out on a clean surface at about 300 K, it is found that the β state is occupied first followed by the α to a saturation coverage ratio, which is obtained only under a 10^{-6}-T CO ambient pressure, of about 3:1 (β to α).[21]

In the ESD of the virgin CO layer, it is found that prolonged electron-beam exposure produces an effect very similar to that of raising the temperature, i.e., the CO^+ decreases and the O^+ increases. These are apparently, however, distinctly different processes.[7,16] In the thermal case, the work function and CO^+ yield fall in a concerted manner while under electron damage it is found that the CO^+ falls rapidly with very little work-function change. After long beam exposures the O^+ signal

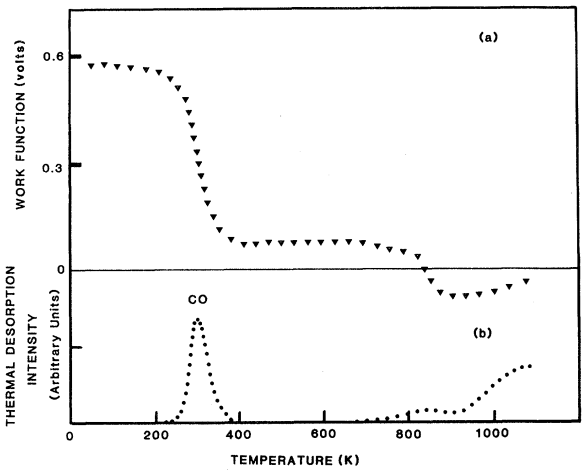

FIG. 12. Data from Gomer (Ref. 7) illustrating (a) the behavior of the work function and (b) the thermal desorption of CO for saturation coverages of CO on the W(110) surface initially exposed at 20 K.

peaks and subsequently diminishes along with the work function.

In addition to the general adsorption-state descriptions, i.e., virgin, α, and β, several other substates have been identified on the basis of their distinct behavior. For example, the α and β states have both been described in terms of substates α_1,α_2 and β_1,β_2,β_3 groups.[22]

B. Discussion of the origins of the O^+ and CO^+ ESD ion yields

It is clear from the brief review above and the results presented here that the large variation in O^+ yield above and below the O 1*s* threshold is a property of the virgin CO adsorption state below 150 K. In addition, the O^+-yield data of Fig. 7 indicate that the effect occurs in this virgin layer only after relative coverages of greater than approximately 0.6 have been reached. Large energy-dependent yield variations disappear from a fully saturated virgin layer in the temperature region where CO desorption is seen (Figs. 9 and 12) and does not begin until relative coverages of about 0.6 are reached (Fig. 7). If, as Steinbruchel and Gomer found,[19] the saturation coverage in the virgin layer is taken to be 0.8 monolayer, then significant variation in the O^+ yield with energy does not begin until coverages of greater than about 0.5 monolayer are achieved. This is the compression region described by Steinbruchel and Gomer where the LEED patterns smoothly change from those indicative of 0.5 monolayer coverage to those indicating 0.8 monolayer. Therefore, it is seen that yield ratio variation is a property of the compresses virgin CO state.

To the authors' knowledge, careful low-energy threshold ESD work on the virgin CO-W(110) system has, as yet, not been done. However, as we mentioned earlier, the overall excitation energy behavior of the O^+ ion yields would seem to imply that there are at least two separate regions where the yield increases from some threshold, peaks, and slowly decreases with increasing excitation energy. Such behavior is common for the electron excitation cross sections for systems having characteristic thresholds and the threshold for these two cross-section curves appear to be below 100 eV for the low-energy behavior and at or above the O 1*s* for the high-energy process.[23] The mechanism by which the low-energy excitation produces the desorption of O^+ and CO^+ is clearly very sensitive to the detailed chemical state of the adsorbed CO. This can be seen in the excitation energy behavior illustrated in Fig. 5, where it is seen that the low-energy O^+ yield is strongly dependent on coverage, and in the fact that low-coverage beam damage dramatically changes the CO^+:O^+ ratio but does not produce significant work function changes.[7,16]

It is interesting to consider in this context whether the O^+ yield corresponding to the O 1*s* excitation shows a similar sensitivity to the binding chemistry of the CO. We can shed light on this question, as outlined earlier, by assuming that the two threshold processes are essentially independent and that the shape of the desorption cross section as a function of energy corresponding to the low-energy excitation does not change as the overall yield changes. This, again, allows us to map the variation of the O^+ yield for each process separately and the results are shown in Figs. 7 and 9.

In both the behavior of the O^+ yield with coverage and post-saturation-coverage annealing, the unique behavior found for the low-energy yield is not found for the high-energy process. In both cases the high-energy behavior more closely follows that of the CO^+ yield. The high-energy O^+-yield value remains constant up to the temperature at which CO^+ begins to decrease (coinciding with the beginnings of CO desorption from the compressed layer),[12] appears to slightly decrease while the low-energy O^+ yield is peaking, and then both fall together for temperatures above 400 K. The fact that the low-energy yield peaks to higher values than those resulting from O 1*s* excitation undoubtedly indicates that the low-energy process has a higher initial-state excitation cross section. *It is appealing to conclude from these data that the high-energy O^+ yield is proportional to molecular CO coverage and not to the detailed adsorption state.*

One possibility for the origin of the low-energy desorption process is that it involves an excitation of the 3σ CO molecular level, i.e., the molecular orbital consisting for the most part pf the oxygen 2*s* shallow-core atomic orbital. Evidence for the involvement of the 3σ excitation in O^+ desorption from adsorbed CO has been seen recently in a photon-stimulated-desorption (PSD) study of CO on Ru(001).[24] In gas-phase dissociation studies, it is found that the C 1*s* and O 1*s* levels are very efficient in the production of C^+ plus O^+ ions as a result of the subsequent Auger decay, giving yields which are enhanced by a factor of approximately 3

over those achieved just below the thresholds.[25] The low-energy C^+ plus O^+ yield increases slowly from an appearance potential at about 24 eV (due to ionization and electronic "shake-up" processes[26]) and reaches a maximum at ~ 50 eV due to excitation from the 3σ states to a final-state σ resonance.[27] At higher energies, the ion yield increases steadily up to the C 1*s* threshold. The 3σ binding energy in CO(*g*) is found to be approximately 38 eV (Ref. 28) and the minimum energy for Auger decay with a CO^{2+} final state appears at about 40 eV.[29] Thus, in the gas phase, conservation of energy prevents Auger decay from the 3σ-level excitation.

Adsorption on a surface, however, gives rise to shifts in the CO levels which make Auger decay from the 3σ excitation possible. In this case the 3σ binding energy is found to be at about 36 eV (Ref. 24) with respect to the metal Fermi level. Auger spectra involving O 1*s* excitation indicates that the minimum energy necessary to permit an Auger decay, i.e., the energy difference between the Auger emission threshold and the O 1*s* binding energy is only about 16 eV.[29] These Auger measurements were made for CO adsorbed at room temperature which is the situation where large O^+ yields are obtained at low energies. Although Ref. 29 reports work on room-temperature CO adsorption on W(110), to our knowledge no photoemission or detailed Auger line-shape work has, as yet, been done on the saturated virgin CO layer on W(110) at temperatures below 150 K. Thus, the mechanism by which the compressed layer suppresses low-energy O^+ yields is still not clear, although a similar behavior has been reported for CO-Ru(001),[30,31] CO-Pd(210),[32] and CO-Ni(111).[33] It could result either from relative orbital energy shifts which make the Auger process unfavorable or give rise to a situation where, even if the Auger event does occur, neutralization is so rapid that the O^+ yield is effectively reduced. The former would seem to be favored by the fact that the CO properties are approaching those of the gas-phase molecule as the virgin layer is compressed, i.e., the CO-metal bond decreases and the CO bond increases in energy. The neutralization model would require that, even though the coupling strength between the CO and metal is decreasing with coverage, the ability of the doubly ionized CO final state to disperse into the metal valence band would increase. This latter model also makes it difficult to explain why the Auger decay from the O 1*s* excitation does not experience a similar increase in neutralization for the compressed virgin layer.

Another aspect of neutralization, which is particularly applicable in the present case, is contained in the recent suggestion of Netzer and Madey that the O^+ yield at high CO coverages may involve significant neutralization by electron hopping from neighboring molecules.[33] Here again, however, it is difficult to understand in this model how the processes differ for the low- and high-energy excitation.

It is not clear at this point, in either case, whether the compressed layer has different properties because of adsorbate-absorbate interactions or because the dense packing forces the occupancy of different adsorption sites. Certainly, the properties of the adsorbate layer must be somewhat altered in the compressed layer due to dipole-dipole interactions or the result of the competition for metal *d* electrons. However, a two-state adsorption model, as discussed previously, would seem to be adequate to explain the various adsorbate properties.[5,12,34,35]

In the context of the ease of low-coverage conversion, it is interesting to note that we find extremely rapid changes in the ESDIAD patterns as a result of electron-induced damage at low coverages which is accompanied by a decrease in the CO^+ and a rise in the O^+ yields.[11,36] The implication in this result is that electron excitation readily converts the CO^+ yielding state to that of a O^+ emitter. We mentioned this sort of behavior earlier along with the observation that a commensurate work-function change was not obtained.[7,16] Thus, at these low temperatures, electron-induced effects apparently readily produce this conversion but do not give rise to the dissociated β state with a large cross section.

The detailed origin of the O^+ and CO^+ yielding states is, as yet, not clear. It is appealing to consider the possibility that the O^+ yielding state is bridge-bonded between two W atoms with an sp^2-type hybridization and the CO^+ yielding states are linearly bonded to a W atom.[7] As modeled by Steinbruchel and Gomer,[19] saturation coverages would certainly force a mixing of these sites. It is also possible that the CO^+ emitting state is due to a more space-filling configuration as, for example, with the axis slightly off normal. This would, perhaps, offset a slight change in hybridization and would represent an appealing precursor state to dissociation. To our knowledge, however, no direct evidence has been obtained to delineate between such detailed bonding models, and no evidence for a tilted CO binding configuration has been found.

If, on the other hand, the diminution in the O^+ yield at the low excitation energies results from a limitation of the phase space available, then this would tend to explain why the O 1*s* excitation does not discriminate between the two states. However, it is difficult to explain on this basis alone why the O^+-ion kinetic-energy distribution for the high-energy excitation extends to lower energies than that for the low-energy excitation. Normally when phase space is a limitation, the higher-energy excitation process would be expected to expand the final-state distributions to higher values.[37] If reneutralization is the key to the excitation energy behavior, then it is difficult to understand why the high-energy excitation causes a reduction in reneutralization rate. At first glance, the curves of Fig. 10(a) would seem to support a reneutralization picture since the low-energy ions are affected to the greatest extent. However, unless opposing effects cause a fortuitous cancellation, it is hard to visualize how reneutralization could be playing a major role without giving rise to a significant energy-dependent isotope effect.

Chemical-state-induced changes in the subsequent reneutralization rate of an adsorbed CO molecule which has been excited to a state that can lead to the emission of O^+ ions is not sufficient to explain the present results. The initial excitation process clearly plays a key role and the fortuitous cancellation mentioned above must involve the excitation probability to the ion-desorbing state and subsequent reneutralization rate.

Note should be taken of the fact that these conclusions concerning the origins of O^+ and CO^+ ion yields differ from those of Weng[13] who associated CO^+ with virgin CO and O^+ with β CO. It appears clear, however, from the present data as well as previous studies[7,12,16,19] that the low-temperature ($T \lesssim 300$ K) O^+ ion yield is due to states *different from* the β state (whose desorption onset is ~ 900 K).

The final resolution concerning the detailed nature of the O^+ and CO^+ yielding states must await careful measurements of the threshold energies for ion desorption over a wide range of temperature and CO coverage; and these measurements can perhaps be best accomplished using photon-stimulated desorption where the threshold behavior is more easily delineated.

V. SUMMARY

In summary, the principal findings of the present work are the following:

(a) The ESD O^+ emission from a saturation virgin CO layer on W(110) at 80 K increases significantly when the incident-electron energy exceeds that necessary to excite the O 1*s* core level.

(b) The low-energy O^+ ion emission (i.e., the ion yield due to excitations below the O 1*s* threshold) exhibits a maximum as a function of CO coverage. The low-energy O^+ yield is sensitive to the detailed chemical bonding structure and to CO-CO interactions at high coverage.

(c) In contrast, the high-energy O^+ ion emission (due to excitations at energies well above the O 1*s* threshold) appears to vary monotonically with CO coverage, and, thus, is less sensitive to the detailed chemical bonding structure.

(d) The low-energy O^+ ion yield for the saturation virgin CO layer increases sharply for temperatures above about 250 K as the excess molecular CO in the compression layer desorbs. In the same temperature range, the CO^+ ion yield decreases with temperature.

(e) The O^+ ion energy distribution for the saturation CO coverage at 80 K excited with low-energy electrons (~ 400 eV) is characterized by a peak energy at approximately 6 eV. For the high-energy excitation (~ 1300 eV), the peak value is shifted down slightly and the distribution extends to considerably lower energies than that found for the low-energy excitation.

(f) For the saturation CO layer at 80 K, the ESD isotopic ratios are found to be

$$I_{^{16}O^+}/I_{^{18}O^+} = 1.67 \pm 0.21$$

$$I_{^{12}C^{16}O^+}/I_{^{12}O^{18}O^+} = 1.26 \pm 0.08 ,$$

and do not show an appreciable energy dependence.

ACKNOWLEDGMENTS

The authors gratefully wish to acknowledge valuable discussions with Professor F. P. Netzer. This work was supported in part by the Office of Naval Research. The work of J.E.H. was performed while visiting the National Bureau of Standards. Sandia National Laboratories is a U.S. Department of Energy facility.

*Permanent address: Sandia National Laboratories, Albuquerque, NM 87185.

[1]M. L. Knotek and P. J. Feibelman, Phys. Rev. Lett. 40, 964 (1978); P. J. Feibelman and M. L. Knotek, Phys. Rev. B 18, 6531 (1978).

[2]M. L. Knotek, V. O. Jones, and V. Rehn, Phys. Rev. Lett. 43, 300 (1979).

[3]T. E. Madey, R. Stockbauer, J. F. van de Veen, and D. E. Eastman, Phys. Rev. Lett. 45, 187 (1980).

[4]See, for example, D. Menzel, Surf. Sci. 47, 370 (1975); T. E. Madey and J. T. Yates, J. Vac. Sci. Technol. 8, 525 (1971).

[5]T. E. Madey and J. T. Yates, Surf. Sci. 63, 203 (1977).

[6]P. A. Redhead, Can. J. Phys. 42, 886 (1964); D. Menzel and R. Gomer, J. Chem. Phys. 41, 3311 (1964).

[7]See, for example, R. Gomer, Proceedings of the 2nd International Conference on Solid Surfaces [Jpn. J. Appl. Phys. Suppl. 2, 213 (1974)].

[8]R. Franchy and D. Menzel, Phys. Rev. Lett. 43, 865 (1979).

[9]K. Besocke and S. Berger, *Proceedings of the 7th International Vacuum Congress and 3rd International Conference on Solid Surfaces, Vienna, 1977,* edited by R. Dobrozemsky *et al.* (IVC, ICSS, Vienna, 1977), p. 893.

[10]T. E. Madey, Surf. Sci. 94, 483 (1980).

[11]T. E. Madey, J. E. Houston, and S. C. Dahlberg, in Proceedings of the 4th International Conference on Solid Surfaces, Cannes, 1980, edited by M. Costa and D. A. Degras [Revue Le Vide—Les Couches Minces Suppl. 201, 205 (1980)].

[12]J. T. Yates and D. A. King, Surf. Sci. 30, 601 (1972).

[13]S. L. Weng, Phys. Rev. B 23, 3788 (1981).

[14]T. E. Madey, J. T. Yates, D. A. King, and C. J. Uhlaner, J. Chem. Phys. 52, 5215 (1970).

[15]C. Leung, C. Steinbruchel, and R. Gomer, Appl. Phys. 14, 79 (1977).

[16]C. Leung, M. Vass, and R. Gomer, Surf. Sci. 66, 67 (1977).

[17]See, for example, L. D. Schmidt, in *Interactions on Metal Surfaces,* Vol. 4 of *Topics in Applied Physics,* edited by R. Gomer (Springer, Berlin, 1975), p. 63; R. R. Ford, Ad. Catalysis 21, 51 (1970).

[18]L. W. Swanson and R. Gomer, J. Chem. Phys. 39, 2813 (1963).

[19]C. Steinbruchel and R. Gomer, Surf. Sci. 67, 21 (1977).

[20]T. E. Madey, J. T. Yates, and R. C. Stern, J. Chem. Phys. 42, 1372 (1965).

[21]J. T. Yates, T. E. Madey, and N. E. Erickson, Surf. Sci. 43, 257 (1974); H. Froitzheim, H. Ibach, and S. Lehwald, Surf. Sci. 63, 56 (1977).

[22]See, for example, J. T. Yates and D. A. King, Surf. Sci. 38, 114 (1973) for a general description and bibliography concerning these states.

[23]R. Jaeger, J. Stöhr, R. Treichler, and K. Baberschke, Phys. Rev. Lett. 47, 1300 (1981), report a delayed threshold at the O 1*s* binding energy in photon desorption of O^+ from CO adsorbed on Ni(100).

[24]T. E. Madey, R. Stockbauer, S. A. Flodstrom, J. F. van der Veen, F. J. Himpsel, and D. E. Eastman, Phys. Rev. B 23, 6847 (1981).

[25]R. B. Kay, P. E. Van de Leeuw, and M. J. Van der Wiel, J. Phys. B 10, 2521 (1977).

[26]R. Locht, Chem. Phys. 22, 13 (1977).

[27]N. Padial, G. Csanak, B. V. McKoy, and P. W. Langhoff, J. Chem. Phys. 69, 2992 (1978).

[28]U. Gelius, E. Basilier, S. Svensson, T. Bergmark, and K. Siegbahn, J. Electron Spectrosc. Relat. Phenom. 2, 405 (1974).

[29]E. Umbach, J. C. Fuggle, and D. Menzel, J. Electron Spectrosc. Relat. Phenom. 10, 15 (1977).

[30]P. Feulner, H. A. Engelhardt, and D. Menzel, Appl. Phys. 15, 355 (1978).

[31]T. E. Madey, Surf. Sci. 79, 575 (1979).

[32]T. E. Madey, J. T. Yates, A. M. Bradshaw, and F. M. Hoffman, Surf. Sci. 89, 370 (1979).

[33]F. P. Netzer and T. E. Madey, J. Chem. Phys. 76, 710 (1982).

[34]J. T. Yates, R. G. Greenler, I. Ratajczykowa, and D. A. King, Surf. Sci 36, 739 (1973).

[35]M. Bowker and D. A. King, J. Chem. Soc. Faraday Trans. 1 76, 758 (1980).

[36]T. E. Madey, J. E. Houston, F. P. Netzer, R. Stockbauer, and D. Hanson, in *Proceedings of First International Workshop on Desorption Induced by Electronic Transitions,* Springer Series in Chemical Physics, edited by N. H. Tolk *et al.* (Springer, Berlin, in press).

[37]R. Locht, Chem. Phys. 22, 13 (1977).